

GRAPHENE SYNTHESIS ON ULTRATHIN METAL CATALYST FILMS

Kaihao Zhang and Sameh Tawfick
 Mechanical Science and Engineering
 University of Illinois Urbana-Champaign
 Urbana, IL

ABSTRACT

Graphene synthesis on ultra-thin catalysts can allow the use of graphene-coated metal films in electronic applications. Graphene coated thin films are expected to offer superior mechanical performance owing to the strength of graphene. However, several factors need to be considered to assure the stability of thin films at the high temperatures required for graphene synthesis. In this work, we present a systematic framework for the selection of thin films (< 1 micron thickness) to be used as catalyst for graphene synthesis. We present our progress towards the rapid synthesis of graphene at 1100°C in less than two minutes, thus avoiding solid state dewetting. The quality of the graphene is assessed by Scanning Electron Microscopy, Raman spectroscopy and indentation. It is shown that these films exhibit higher stiffness and resistance to crack propagation.

Keywords: graphene, synthesis, chemical vapor deposition, thin films, mechanics.

INTRODUCTION

The structure of thin conductive metal films, such as gold, silver, platinum or palladium, deposited by sputtering or e-beam evaporation, are characterized by ultra-small grains. The grain size is typically on the order of the film thickness of a few hundreds of nanometers. While these films are suitable for use in microelectronics, their grain structure affects their mechanical behavior, which has implications on their use in flexible electronics. In these applications, the thin films are subject to cyclic mechanical stresses due the flexible and bendable nature of these devices. These stresses could eventually lead to the failure of these films due to fatigue and crack propagation.

Graphene, a two-dimensional lattice of sp^2 -hybridized carbon atoms, has outstanding mechanical strength. Its electronic properties depend on its interaction with the underlying substrate, but the electron mobility is generally high in graphene having low defect density. Several composites take

advantage of the strength of graphene and have demonstrated enhanced yield strength and synergistic toughening.

It is expected that graphene can reinforce thin metal films for use in flexible electronics. However, for this strengthening to be effective, graphene must have a clean strong interface to the metal. This clean and strong interface is challenging to achieve by transferring the graphene from the growth substrate to the metal thin films due to residues at the interface, and to out-of-plane wrinkling of the graphene.

An alternative approach would be the direct Chemical Vapor Deposition (CVD) based synthesis of graphene on thin metal films which can then be directly used in flexible electronics. CVD of graphene has seen tremendous developments in recent years, leading to the successful synthesis of large domain size high quality monolayer graphene. Several catalysts are used for synthesis including copper, platinum and nickel.[1] The role of the catalyst is to catalyze the dehydrogenation reaction of the hydrocarbon gas, such as methane, and to allow the mobility of the carbon atoms and their crystallization into graphene layers. However, these reactions take place at high temperatures which could lead to metal solid state dewetting. Thin metal films are unstable at high temperatures. Metals tend to minimize their free surface energy by solid state dewetting. Dewetting is driven by several processes including grooving at the grain boundaries and triple junctions, hole formation, edge retraction and fingering instability.[2] Nanometer thin film breaks into discrete islands at temperatures as low as one half of the melting temperature of the corresponding bulk metal, and challenges graphene synthesis since most CVD processes require long duration at temperatures significantly higher than the onset of dewetting. Moreover, synthesis of graphene on sub-micron thin catalysts is also challenged by the carbon atoms diffusion kinetics because it takes much shorter duration to saturate thin film catalysts compared to thick foils having $> 10 \mu\text{m}$ thickness. The extreme thinness limits the flux of carbon from the gas into the bulk of the catalyst typically leading to multi-layered graphene growth.

Table 1. Thin metal films for use in graphene CVD

Metal-Gr	Lattice of metal (111) [Å]	Mismatch	Binding energy [meV/atom]	Separation distance [Å]	Normal stress [GPa]	Adhesion energy [J/m²]	Resistivity [nΩ·m]	Young's modulus [GPa]	Melting point [°C]	Carbon solubility at 1000°C	Comments
Gr-Gr	2.461		0.5	3.24		0.35					↓interaction
Cu-Gr	2.543	3.3%	33	3.3	2.92	12.8	16.75	120	1084	0.04	↓interaction
Pt-Gr	2.766	12.4 %	38	3.3			105	168	1768	1.43	↓interaction
Ni-Gr	2.474	0.5%	125	2.1	18.7	72.7	63	200	1455	2.04	↑interaction oxidation
Pd-Gr	2.729	10.9 %	84	2.5			105	121	1554	6.11	↑interaction

MATERIAL SELECTION

We have considered several factors to select the most suitable thin films for graphene synthesis (see Table 1).[3] The metal film needs to be effective catalyst for graphene synthesis but should have high enough melting temperature to resist solid state dewetting at 1100°C. For example, copper is automatically excluded due its low melting temperature which makes it impossible to synthesize highest quality graphene (~1100°C) on extremely thin metal ligaments without melting it. Ni, Pt and Pd are both attractive owing to their high melting temperature. Another extremely important consideration for the following analysis is the binding strength between the metal and the graphene. In general, it is known that metals can be categorized into two groups based on how strong they bind to graphene. Pd and Ni belong to the strongly binding group and as a result they both represent the first choices use as the thin film metal catalyst.

MODELING

We use analytical modeling to demonstrate that the strength and toughness, owing to the strong interaction of the graphene on these metals, do not follow rules of mixtures. Huge enhancements can be obtained for these materials including three orders of magnitude enhancements in the toughness. A cross section of the material proposed here has a periodic arrangement of metals coated with atomically-registered graphene, with ligaments separated by small air gaps. The half-period is $\lambda = (\#_{Gr} t_{Gr} + t_m)/2$ where $\#_{Gr}, t_{Gr}$ are the number of layers and thickness of the graphene and t_m the metal thickness be it Pd or Ni. The average elastic constant E is $E_{Gr|m} = \frac{E_{Gr}\#_{Gr}t_{Gr}+E_m t_m}{\#_{Gr}t_{Gr}+t_m}$ and it is synonymous to the composite elastic constant made of stacks of *graphene* and *metal* layers. The enhancement in the elastic properties of the metal film with graphene on the surface can be described by $\kappa_{Gr|m} = 1 - E_{Gr|m}/E_{Gr}$ where $E_{Gr} = E_{max}$ is the maximum modulus or the stiffer material in the composite. While calculating the average elastic modulus of the material is straightforward, the strength and fracture properties are much more involved as well as interesting, due to their intimate layered structure. For example, it is known that biological materials such abalone shells and bones have fracture strength and toughness far exceeding their individual constituents due to their layered morphology. The mathematical analysis adopted

here is similar to that of biological layered materials also exhibiting strong interfacial binding energy resembling the proposed atomically registered graphene. The analysis considers many ligaments wrapped with graphene and having small defects in the form of sharp penny-shaped holes, which allows the application of the Griffith criterion. Notably, this simple analytical criterion has been applied to graphene and other nanomaterials which exhibit brittle fracture.[4]

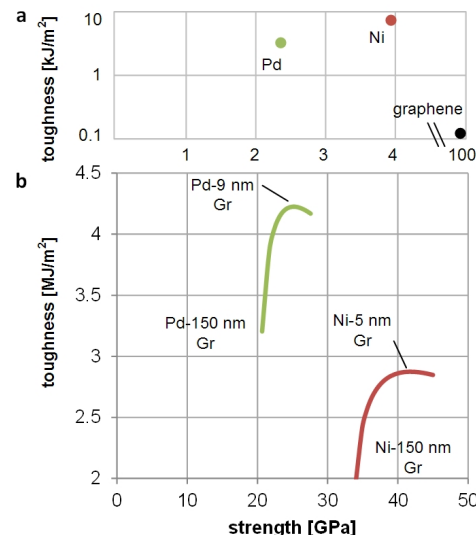


Figure 1. Calculated properties of the graphene reinforced thin metals. a) Toughness Vs. strength of the single elements of the proposed material (Ni/Pd nanowires and high-quality graphene sheets); b) Toughness (note MJ/m² units) Vs. strength of the proposed materials exhibit optimum toughness values at 9 nm Pd core and 5 nm Ni core; while the strength keeps increasing as the metal core size is reduced, where the wrapped graphene dominates the response. Note that the toughness does not obey rules of mixture of plot (a) values.

When graphene has high binding energy on Pd or Ni, their fracture strength is $\sigma_{Gr|m} = \sigma_{Gr}(1 - \kappa_{Gr|m}) \sqrt{\frac{1}{\psi} \frac{2a_n E_{Gr}}{\lambda E_m}}$ where ψ is a geometric parameter equal to 5 when $t_m \gg \#_{Gr} t_{Gr}$ and $2a_n$ is the critical defect size in the metal-graphene assembly. [5]

The terms on the right hand side are by definition smaller than 1, indicating that the material is weaker than free standing graphene layers. Toughness is a measure of how much energy is dissipated as crack propagates through the material, and it is measured by fracture energy which is the energy required to create the surfaces of a crack (J/m²). It can be shown that for a layered material $J_{Gr|m} = H \left(\frac{W}{\lambda}\right)^{\frac{2}{M}} \frac{\sigma_{Gr}^2}{E_{Gr|m}}$ where H and W are the ligaments height and width respectively, and M is the Weibull modulus, which for 2D materials (e.g. *Gr*) is ~ 10 .[6]

This relation shows that the proposed material will always be tougher than *graphene* by the factors $\left(\frac{W}{\lambda}\right)^{\frac{2}{M}}$ and $\frac{1}{E_{Gr|Pd}}$ both of which are $\gg 1$. [7] This relation is computed for variable $\#_{Gr} t_{Cr}/t_m$ ratios and the results are plotted in **Figure 1**. This plot clearly depicts the toughness superiority of graphene coated thin films with vastly different stiffness, namely $E_{Gr|Pd}$. Additionally, consistent with the fracture strength results, the toughness is significantly enhanced as the number of layers is decreased. The proposed material can reach values of a few MJ/m² which is 100 times tougher than the toughest metals.

SYNTHESIS APPROACH

Graphene synthesis on transition metals such as Pd and Ni, which are the focus of this study, rely on their high carbon dissolution capability as shown in **Figure 2**. During the synthesis step, the hydrocarbon (CH₄) dissociates into carbon atoms and dimers. The resulting carbon atoms diffuse into the bulk of the lattice. It is now established that although some nucleation may occur during this step, most of the graphene growth takes place during cooling. Considering the solid-state dewetting of thin films at synthesis temperatures, catalysts need to be retracted for cooling before being saturated with carbon atoms. As temperature drops during cooling, carbon diffusion from gas to catalyst can continue while the precipitation of dissolved carbon to the catalyst surface may occur. As a result, as expressed in Figure 2c and Figure 2d, the cooling rate (cooling duration) and hydrocarbon gas concentration control the concentration of carbon on the surface. This step accordingly controls the quality, crystal size and number of layers of graphene.[8]

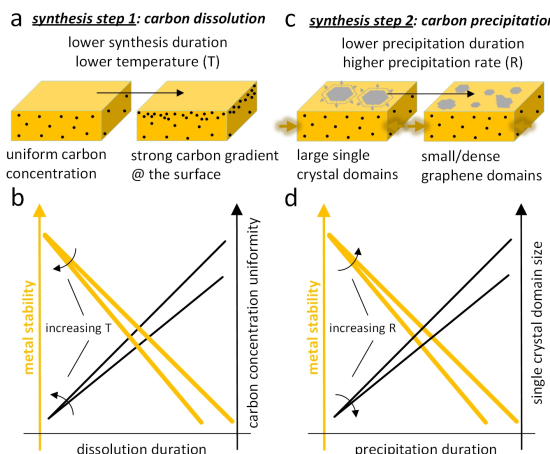


Figure 2. Steps and trade-offs involved in the synthesis of graphene on a thin metal. (a) Schematic of the carbon dissolution step and the resulting uniformity of carbon dissolution in the catalyst; (b) trade-offs on metal instability and carbon uniformity; (c) Schematic of the carbon precipitation step responsible for the growth of the carbon domains; and (d) trade-offs on metal stability and quality of graphene.

SYNTHESIS RESULTS

In this study, we focus on Pd catalyst due to (i) its high melting point and hence resistance to dewetting, (ii) its strong catalytic activity, (iii) high resistance to oxidation compared to Ni and (iv) commercial availability in the form of 100 nm leaves. **Figure 3** illustrates the fabrication processes of Pd-Gr composite leaves. Commercially available Pd leaves, shown in Figure 3a, come in a booklet of freestanding sheets separated by low surface energy paper.[8] Scanning electron microscope (SEM) imaging (Figure 3b) shows the Pd grain structure. The average grain size is 20 μm and extends through the film thickness. Commercially available thin Pd leaves have large grains and we previously found that they are suitable for synthesis compared to thin film made by e-beam evaporation or sputtering. A freestanding Pd leaf is typically laminated on a SiO₂/Si substrate and annealed at 500 °C for 5 hours, as sketched in Figure 3c. The annealing step releases the residual strains associated with the lamination of the Pd leaf on the substrate. After annealing, the substrate supporting the Pd leaf is removed from the furnace using a transfer arm. The furnace temperature is then increased to the synthesis temperature of 1100 °C. When furnace temperature T_f stabilizes at 1100 °C, CH₄ (50 sccm) is introduced 10 min before the Pd is inserted in the hot zone for a short duration. During the growth, the vacuum is maintained at 1.72 Torr. The substrate is then rapidly retracted out of the hot zone at a velocity of 0.5 m s⁻¹ while maintaining a controlled flow of CH₄ and He gas mixture during cooling. The crystalline graphene domains grow epitaxially over several microns, can traverse the metal grain boundaries, and merge with neighboring crystals to cover the whole leaf. SEM (Figure 3d) taken at the edge of the film clearly shows hexagonal shaped graphene domains ($\theta = 120^\circ$) on the surface of the Pd leaves, where the graphene exhibits a darker region in the SEM. The Raman spectrum of graphene on Pd is characterized by a weak signal to noise ratio, which is similar to the spectra of monolayer graphene on other highly binding metals such as Ni. The electrochemical “bubbling” method can be successfully used to transfer the graphene from the Pd leaf to SiO₂/Si substrate. Figure 3e shows a typical Raman spectrum for the transferred graphene sheet, with intensity ratio of 2D/G around 4.3 and 2D peak (~2676.4 cm⁻¹) that is well fitted by a single Lorentzian function with a FWHM of ~30.1 cm⁻¹. Figure 3f is the histogram of D/G ratio from a Raman map of a 23 μm × 23 μm region, comprising several graphene grains, with a mean value less than 0.08, suggesting the low defect density of the graphene monolayer, even after the severe manipulations associated with transfer. After synthesis, the Pd-Gr composite leaf can be readily delaminated from the SiO₂/Si substrate by slowly submerging it into water, due to the wettability of the surface by the water molecules.

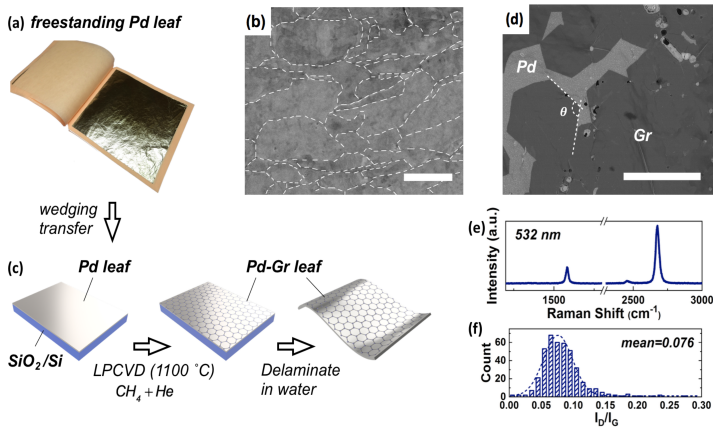


Figure 3. Fabrication of Pd-graphene (Pd-Gr) leaves by low pressure chemical vapor deposition (LPCVD). a) Pd leaves ($140\text{ mm} \times 140\text{ mm} \times 150\text{ nm}$) are commercially available as freestanding sheets laminated between low surface energy paper. b) Scanning electron microscope (SEM) image of the as-received Pd leaf. The dashed lines outline the grain microstructure of the leaves (average grain diameter $\sim 20\text{ }\mu\text{m}$). Scale bar: $15\text{ }\mu\text{m}$. c) A Pd leaf is conformally laminated on SiO_2/Si substrate using the capillary forces of a water film, cleaned and annealed in He at 500°C for 5 hours. Graphene is synthesized on Pd leaf by LPCVD at 1100°C , 1.79 Torr, with CH_4 and He gas mixture for 30 s. After synthesis, the Pd-Gr leaf can readily delaminate from the substrate by immersing in water, leaving a freestanding sheet. d) SEM image of monolayer graphene on Pd leaf near the boundary of fully covered leaves, showing the crystalline hexagonal graphene grains. Scale bar: $50\text{ }\mu\text{m}$. e) Raman spectrum (532 nm laser) of the as-grown graphene sheet after separation from the Pd and transfer to a SiO_2/Si substrate. f) Histogram of the D- to G-peaks intensity ratios obtained from Raman maps ($23\text{ }\mu\text{m} \times 23\text{ }\mu\text{m}$) showing the low defect density of the graphene.

Mechanical Behavior TESTING

We have tested the mechanical behavior of the Pd-graphene films by strip indentation. We transfer freestanding Pd-graphene films to TEM grids and use a wedge indenter to determine their young's moduli. To be able to measure properties from the nonlinear indentation force-displacement response, various fitting ranges have been tested as shown in Figure 4.

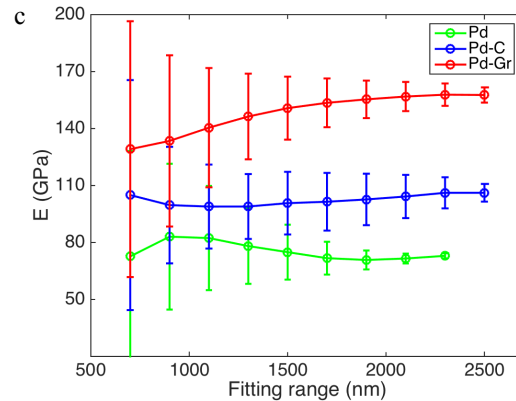
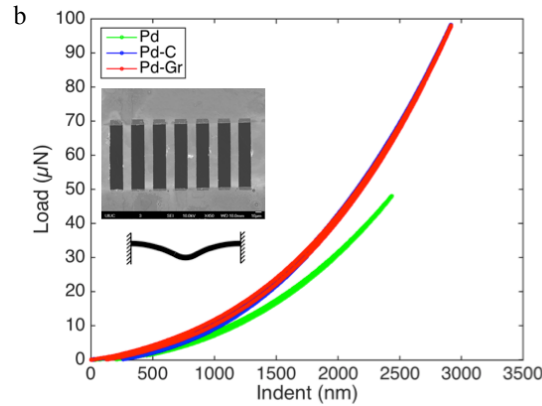
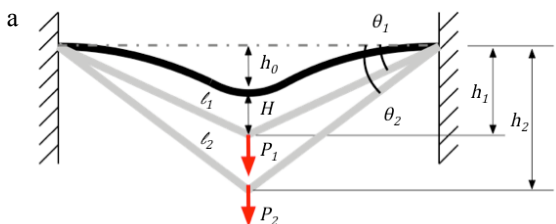


Figure 4. Strip indentation results of Pd leaves, and Pd-graphene leaves. a) Schematic of nanoindentation model for a slack freestanding strip. b) Force-displacement curves of bare Pd leaf, as-grown Pd-graphene and Pd-C (palladium carbide) by etching the graphene from the Pd-graphene samples using oxygen plasma. c) Comparison of elastic moduli of Pd, Pd-graphene and Pd-C.

We derived a force-displacement relation that takes into consideration any slack in the length of the strips. This new relation is

$$P = \frac{8AE}{l_0^3} h^3 + \frac{24AEh_0}{l_0^3} h^2 + \left(\frac{4AE}{l_1} + \frac{24AEh_0^2}{l_0^3} - \frac{4AE}{l_0} \right) h + f(h_0)$$

$$f(h_0) = \frac{8AE}{l_1} h_0^3 + \left(\frac{4AE}{l_1} - \frac{4AE}{l_0} \right) h_0$$

where P is the load, E is the Young's modulus, h , and l are as shown in Figure 4.

The trends shown in Figure 4 are for various fitting parameter. It can be observed that there is a lot of scatter in the data when the fitting range is smaller than 1500 nm. The moduli extracted from larger fitting range have less scatter and the values reach a final stable mean. We can hence conclude that the modulus of Pd-Gr and Pd are 155 GPa and 80 GPa respectively. We also etched the graphene from the Pd-Gr

samples to check if the Pd stiffness increased during CVD due to carbide formation. Indeed, the Pd-C (carbide containing films) have an increased modulus of 108 GPa. Note that this modulus is for the composite films (Pd+Gr). We conclude that several factors contribute to the increase in modulus observed for the Pd-Gr films including the stiff carbide, residual stresses at the Pd-C/Graphene interface and increase in surface modulus of that interface. Detailed studies to quantitatively relate the origins of strengthening to these phenomena will be carried out in the future.

Finally, we use the strip indentation method to observe the crack patterns in Pd versus Pd-Gr films. We use Focused Ion Beam to make notches in suspended Pd and Pd-Gr thin films. These notches concentrate the stresses at the notched areas and lead to fracture as shown in Figure 5.

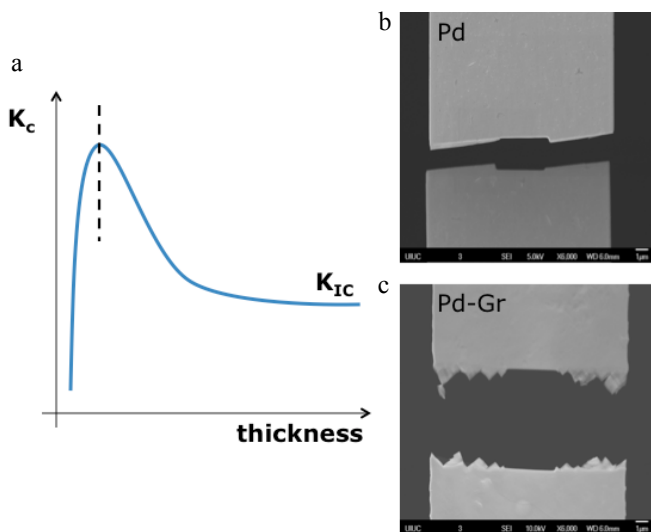


Figure 5. a) Fracture behavior of thin films is shown schematically. SEM images showing the difference between the fracture behavior of b) Pd and c) Pd-Gr.

While metals are generally known for their high toughness due to their ductility, thin films suffer low fracture toughness (K_c) as shown in Figure 5. In fact, the fracture toughness of thin films is typically lower than plane strain fracture toughness (K_{IC}). This can be attributed to many factors such as strain localization and the rapid nucleation of cracks when the film thickness is on the same order of the grain size.

While we have not measured the exact values of fracture toughness at this point, we have qualitative results indicating extreme toughening phenomena. Indeed we have observed that the Pd thin films exhibit brittle fracture as shown in Figure 5. This can be concluded by the straight crack morphology emerging from the notches made by FIB. On the other hand, we have observed that the Pd-Gr thin films exhibit saw-tooth like crack morphology, which is indicative of higher toughness. A serrated crack morphology is often observed when significant

ductile behavior is present in cracks. It can be qualitatively explained as follows: the cracks follow the direction of the maximum shear stress which is oriented at 45° due to the plane stress nature of the stress state in thin films. However, if the crack propagation is stable and the material is ductile, significant work hardening takes place in the metal ahead of the crack tip. Once sufficient strain hardening occurs, the crack changes direction from +45° to -45°, thus following the other maximum shear stress direction. This process keeps repeating and a saw-tooth crack propagation pattern is observed.

CONCLUSIONS

We have demonstrated a new concept of synthesizing graphene by CVD on thin films to enhance their mechanical behavior. We presented a systematic approach to select metal catalyst suitable for graphene synthesis on thin films. We have demonstrated a rapid CVD synthesis approach to coat thin films of 100 nm thickness with graphene. We used strip indentation to measure the elastic modulus of the coated films, and we qualitatively observed the fracture patterns of these films to assess their fracture toughness. In the future we will quantitatively relate the modulus increase to the surface modulus of the Pd-Gr, residual stresses at that interface and carbide formation. We will also measure the fracture toughness of these films and their electric properties towards their use in flexible electronics having higher crack resistance.

ACKNOWLEDGEMENT

We acknowledge the support by the Office of naval Research grant N00014-15-1-2469 and N00014-18-1-2457.

REFERENCES

- [1] A. Dahal, M. Batzill, "Graphene-nickel interfaces: a review," *Nanoscale*, vol. 6, pp. 2548-2562, 2014.
- [2] C.V.Thompson, "Solid-State Dewetting of Thin Films," *Annual Review of Materials Research*, vol. 42, pp. 399-434, 2012.
- [3] S. J. Chae, F. Güneş, K. K. Kim, E. S. Kim, G. H. Han, S. M. Kim, H.-J. Shin, S.-M. Yoon, J.-Y. Choi, M. H. Park, C. W. Yang, D. Pribat, and Y. H. Lee, "Synthesis of Large-Area Graphene Layers on Poly-Nickel Substrate by Chemical Vapor Deposition: Wrinkle Formation," *Advanced Materials*, vol. 21, pp. 2328-2333, 2009.
- [4] P. Zhang, L. Ma, F. Fan, Z. Zeng, C. Peng, P. E. Loya, Z. Liu, Y. Gong, J. Zhang, and X. Zhang, "Fracture toughness of graphene," *Nature communications*, vol. 5, 2014.
- [5] O. Kolednik, J. Predan, F. D. Fischer, and P. Fratzl, "Bioinspired Design Criteria for Damage-Resistant Materials with Periodically Varying Microstructure," *Advanced Functional Materials*, vol. 21, pp. 3634-3641, 2011.

- [6] A. Shekhawat and R. O. Ritchie, "Toughness and strength of nanocrystalline graphene," *Nature communications*, vol. 7, p. 10546, 2016.
- [7] O. Kolednik and L. Nicolais, "Fracture Mechanics," in *Wiley Encyclopedia of Composites*, ed: John Wiley & Sons, Inc., 2011.
- [8] K. Zhang, C. Androulidakis, M. Chen, and S. Tawfick, "Gilding with Graphene: Rapid Chemical Vapor Deposition Synthesis of Graphene on Thin Metal Leaves," *Advanced Functional Materials*, vol. 0, p. 1804068.